



Detailed survey on minimum activation energy for penetration of Ni nanoparticles into Bi-2223 crystal structure and temperature-dependent Ni diffusivity

Yusuf Zalaoglu¹ · Cabir Terzioglu² · Tahsin Turgay³ · Gurcan Yildirim⁴

Received: 4 October 2017 / Accepted: 11 November 2017 / Published online: 17 November 2017
© Springer Science+Business Media, LLC, part of Springer Nature 2017

Abstract

The primary contributions of this study are not only to explore the role of diffusion annealing temperature interval 650 to 850 °C on the formation of effective electron–phonon coupling or cooper-pair probabilities (percentage of clusters in the superconducting path), densities of active and dynamic electronic states at Fermi energy level, stabilization of superconductivity in the homogeneous regions, overlapping of Cu-3d and O-2p wave functions and bond strengths in the crystal matrix of Ni surface-layered Bi-2223 polycrystalline ceramics, but also to determine the temperature-dependent diffusion fast-rate and required minimum activation energy for the diffusion of Ni foreign impurities into the bulk Bi-2223 superconducting crystal structure for the first time. The dc electrical measurement results obtained show that the optimum diffusion annealing temperature is found to be 700 °C for the penetration of optimum Ni concentration into the Bi-2223 crystal lattice so that the ceramic compound exposed to 700 °C annealing temperature exhibits the highest electrical and superconducting properties. In this respect, the material with the minimum electrical resistivity parameters of $\Delta\rho$, ρ_{115K} , ρ_{res} and ρ_{norm} obtains the maximum superconducting characteristics of T_c^{onset} , T_c^{offset} and RRR . Accordingly, the annealing temperature of 700 °C promotes the Bi-2223 ceramics for usage in the engineering, electro-optic, industrial and large scale applications. At the same time, the diffusion coefficients [$D = D_0 \exp(E/k_B T)$] determined at annealing temperature ranging from 650 to 850 °C are observed to be much more significant at rather higher temperatures as compared to lower temperatures. The temperature-dependent Ni diffusion coefficient is determined to be $D = 3.9707 \times 10^{-7} \exp[-1.132 \text{ eV}/k_B T]$ for the Bi-2223 particulate solid material. Namely, the diffusion coefficient is calculated to be about $3.9707 \times 10^{-7} \text{ cm}^2 \text{ s}^{-1}$ when the required minimum activation energy for the introduction of heavy metal Ni ions to the bulk Bi-2223 crystal structure is computed to be about 1.132 eV, being one of the most striking points deduced from this work.

1 Introduction

Throughout the history of superconducting materials, the interest has enhanced constantly due to their own intriguing and developing properties as regards largely higher magnetic

field and current carrying capacity, extremely small energy losses, dissipations and power consumption [1–3]. Type-I and type-II are accepted to be two fundamental classes for the superconducting compounds. The superconductivity era begins with the discovery of type-I materials while the high-temperature cuprates (type-II compounds) described as the ceramics are composed of the perovskite structures with the Cu–O₂ consecutively stacked layers [4, 5]. Hence, the latter materials exhibit different phases with regard to the stacked layer numbers in the unit cell. The type-II compounds crystallize in the tetragonal crystal system except for the Y-based superconducting ceramic compound that obtains the orthorhombic crystal structure and Cu–O chains [6, 7]. It is another difference between the type-I and type-II compounds that the ceramic compounds with easier and faster phase formation, lower material cost and easier availability of the starting powders, environmental benefits,

✉ Yusuf Zalaoglu
yzalaoglu@osmaniye.edu.tr

¹ Department of Physics, Osmaniye Korkut Ata University, 80000 Osmaniye, Turkey

² Department of Physics, Abant Izzet Baysal University, 14280 Bolu, Turkey

³ Department of Architecture, Sakarya University, 54187 Sakarya, Turkey

⁴ Department of Mechanical Engineering, Abant Izzet Baysal University, 14280 Bolu, Turkey

inexpensive and innocuous chemical contents seem to be the focus of attention for the potential industrial applications [8, 9]. Moreover, the ceramic materials have easier been adapted to the application-oriented material science, industrial, metallurgical, and technological as compared to the ordinary conductors and type-I superconductors. Similarly, the cuprates are promising candidates for the practical and engineering applications as a consequence of the considerable decrease in the weight and size of motor, generator and supporting equipment for the production processes [10–12]. Furthermore, the intrinsic optical, electronic and magnetic performances give a direct to the type-II ceramics for the usage in the theoretical modelling studies, electro-optics, heavy-industrial technology, future renewable energy systems and large scale application fields [13–17]. On the other hand, the fundamental usage problems (serious obstructions) such as the narrow operating temperature ranges, excessive brittleness towards the applied loads, sensitivity against the magnetic field and current as well as the inherit physical problems including the structural layers, default (random distribution) of the grain connectivity coupling, large penetration depths low charge carrier densities, and short coherence lengths limit the usage of type-II ceramic materials in the new applications of scientific and electric power equipments [18, 19]. Different production procedures such as the change of preparation materials and conditions (dopant type/quantity, composition, operational procedure, calcination/annealing ambient environment, heat-treatment including pressure, time and temperature) and the altered crystalline structure by the chemical doping/substitution/addition into the system, transition metal diffusion onto the sample surface enable the handicap properties given above to overcome the limitations in the novel applications (to amend the physical problems) of the type-II superconducting ceramics [20–23]. Foremost among the production procedures, the transition metal diffusion takes the lead as a consequence of simple and easy reproducible to prevent the restrictions of ceramic materials [24]. However, the thoroughly understanding of diffusion mechanism is hard phenomenon due to its intrinsic physical and mathematical quantities. Accordingly, in this part we need to explain the mechanism with the related quantities in more details.

Diffusivity (directly related to the diffusion fast-rate or diffusion coefficient) is interested in not only how the impurity particles diffuses or separates throughout the pore space of porous media but also how fast the foreign atoms penetrate into the crystal structure [25]. The term is the proportionality constant between the molar flux (known as the movement of impurity from high concentration region to low concentration region = Fick's first law) and the gradient in the impurity concentration. Moreover, the transfer (movement) rate of particles across a unit area paves way to gather the information about the environment concentrations.

Accordingly, the impurity more rapidly diffuses into the target material with the increment of the gradient difference or diffusion fast-rate. There are many useful available relations in the physical chemistry to describe the diffusivity of any solid impurity material through the crystal lattices. Foremost among the relations, the equations based on the Fick's laws become the leaders for the solutions of exchange rate of a gas across a fluid membrane, radiation transfer, neurons, pharmaceuticals, biopolymers, porous soils, population dynamics, nuclear materials, semiconductor and superconducting substitution/addition/doping process, hydraulic flow, model transport processes in foods, charge and heat. Furthermore, the diffusion equation of Fick's second law delves strongly into the innovative and novel technological products deduced from the integrated circuit fabrication technologies and model processes such as the chemical vapor deposition, physical vapor deposition, thermal oxidation, wet oxidation, addition, substitution and doping. The long and short of it is that the Fick's Laws are responsible for the best understanding of diffusion mechanisms in the solids, liquids and gases. In this respect, the four main methods from the application of Fick's second law can be used to define the diffusivity of the superconducting compounds,

- (i) Radio tracer,
- (ii) EDXRF,
- (iii) Variation of the lattice cell parameters deduced from the XRD experimental results after the successive removal of thin-layers on the specimen surface,
- (iv) Change of resistivity/conductivity after removal of thin-layers on the sample surface.

The first two methods (radio tracer and EDXRF) consisting of the expensive procedures are scarce for the scientific studies although the other methods (iii and iv) exhibit the similar and closer results. Besides, the latter methods (especially the fourth one) enable us to collect the reliable results for the diffusivity of any foreign impurity into the crystal structure. In the present study, the diffusion fast-rates of nickel foreign impurities throughout the bulk Bi-2223 superconducting crystal system (received as the diffusion space) are found at the different diffusion annealing temperatures ($650 \leq T \leq 850$ °C) by using the dc electrical resistivity variations as a function of the thin-layer removal from the specimen surface with the aid of error function. The temperature-dependent diffusion coefficient parameter being interested in the relation between the Ni diffusion coefficient and annealing temperature is calculated by use of the mean diffusion fast-rates determined. At the same time, the required minimum activation energy for the penetration of Ni impurities into the bulk Bi-2223 crystal lattice is computed by the Arrhenius equation for the first time. Thus, this study develops a strong methodology between Ni impurity

concentration in the Bi-2223 crystal system and the crucial characteristics of ceramics such as the electrical, superconducting and structural properties. Further, to the best of our knowledge, so far there has been no detailed research on either the temperature-dependent diffusion coefficient or required activation energy for the introduction of Ni nanoparticles to bulk Bi-2223 superconducting ceramics, being one of the most striking point inferred from this work.

2 Experimental measurement details and computational approaches

The experimental details related to the sample preparation procedures as well as the variation in structural, superconducting, flux pinning and mechanical properties of the Ni surface-layered bulk Bi-2223 superconducting materials produced by the conventional solid-state reaction method at different diffusion annealing temperature changing between 650 and 850 °C were previously provided in Ref [26, 27]. In the current study, we focus not only on strongly the changes of electrical and superconducting properties of Ni surface-layered Bi-2223 ceramic materials in more detail by means of the dc resistivity measurements, but also on the description of nickel diffusion fast-rate (coefficient) and required activation energy for the penetration of nickel impurities into the Bi-2223 crystal lattice for the first time. For the first part, dc electrical resistivities are measured from the sample surfaces under 5 mA dc current. We record the experimental dc electrical resistivity values against the temperature range of 90–115 K with the aid of the four-point contact method by using Helium closed-cycle cryostat system (provided from CRYO Industries) with provision for the vacuum. Every contact is covered by the silver paint to avoid the extra contact resistance. The experimental signals within the temperature accuracy of about ± 0.01 K are collected by the combination apparatus of a Keithley 2700 nano-voltmeter and a Keithley 220 programmable current source controlled by LabVIEW computer program. Onset critical transition temperatures (T_c^{onset}) are evaluated from the superconducting transition of isolated grains (related to the intragrain region) when offset critical transition temperatures (T_c^{offset}) are deduced from the inter-granular regions. The other electrical characteristic parameters as regards the room temperature resistivities (ρ_{300K}), residual resistivities (ρ_{res}), residual resistivity ratios (RRR), ρ_{115K} , ρ_{norm} , and $\Delta\rho$ are also extracted from the dc electrical curves. For the second part of the study, the change of specimen resistivity after the successive removal of thin-layers of about 10–150 μm from the material surface layered Ni ions allows us to easily calculate the physical quantities given above. One can observe the detailed calculation methods below for the determination of temperature-dependent diffusion fast-rate (coefficient) and required

activation energy value of the Ni impurity for the Bi-2223 superconducting crystal system.

The diffusion equation (Fick's second law) is the derivation of Fick's first law (the diffusive flux) and is used to define how the concentration of species changes with the time. The diffusivity can be obtained from the solution of partial differential equation in one-dimension by using quick approximation of complementary error function [28]. In this study, through the computations for temperature-dependent diffusion coefficient, the Ni impurity diffusion is accepted to move from a constant source into a semi-infinite solid (diffusion space). In other words, the Ni impurity begins at 0 at the surface and spreads infinitely deep in the material [29]. Namely,

$$N(x_0, t) = N_0 \left[1 - \text{erf} \left(\frac{x}{2\sqrt{Dt}} \right) \right] \quad (1)$$

here the diffusion length of $2\sqrt{Dt}$ displays a measure of how far the impurity concentration can propagate in one-direction by the diffusion in the certain time of t [30]. Moreover,

$$\text{erf} \left[\frac{x}{2\sqrt{Dt}} \right] \text{ points out the error function connected with } y = \left[\frac{x}{2\sqrt{Dt}} \right] \quad (2)$$

$$\text{erf}(y) = \left(\frac{2}{\sqrt{\pi}} \right) \int_0^y \text{erf}(-y^2) \quad (3)$$

3 Results and discussion

In our research for the current paper, we advance in-depth understanding of not only two fundamental physical quantities as regards diffusion coefficient and corresponding activation energy of Ni foreign impurities throughout the Bi-2223 superconducting crystal system but also crucial changes in the electrical and superconducting characteristics of the Bi-2223 polycrystalline ceramics exposed to the evaporation of Ni inclusions on one surface of the materials. In the first part of the paper, we are directly interested in both the experimental electrical resistivity measurement results of the pure and Ni surface-layered Bi-2223 cuprate ceramics annealed at different diffusion temperatures in a range of 600–850 °C, and the deduced parameters regarding the critical onset/offset critical transition temperatures, residual resistivities (ρ_0), normal state temperature resistivities at 300 K (ρ_{300K}), residual resistivity ratios (RRR), $\Delta\rho$ and ρ_{norm} parameters. At the end of the paper, we determine the temperature-dependent diffusivity by means of the

resistivity changes against the thin-layer removal from the specimen surface and required minimum activation energy value for the nickel impurities along with the polycrystallized Bi-2223 superconducting crystal lattice by using the Arrhenius relation for the first time.

3.1 Experimental dc electrical resistivity measurement results

In this part of paper, we survey centrally the influence of nickel foreign nanoparticles embedded in the Bi-2223 crystal structures (annealed at different diffusion temperatures of 650–850 °C) via the variation of dc electrical resistivity values versus the temperature ranging from 90 K until 115 K. The experimental dc electrical resistivity results measured are graphically gathered in the inset of Fig. 1. One can also show the normalized resistivity curves in the same figure to easier investigate the influence of diffusion annealing temperature ($650 \leq T \leq 850$ °C) on the dc electrical resistivity measurement results. According to the inset of figure, initially, the conductivity tends to enhance with the annealing temperature and in fact reaching the global maximum point in case of the critical annealing temperature value of 700 °C. However, from higher annealing temperature such a value of 700 °C onwards, the electrical resistivity suddenly increases as a result of differentiation of conducting mechanism in the crystal system. In more detail, the deduced parameters regarding the offset–onset critical transition temperatures, normal state resistivities at room temperature of 300 K (ρ_{300K}), residual resistivities (ρ_0), residual resistivity ratios (RRR), ρ_{115K} , ρ_{norm} and $\Delta\rho$ parameters enable us to determine the role of annealing temperature on the nature

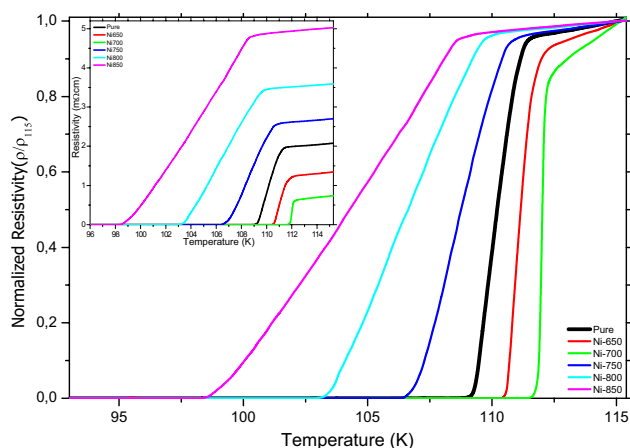


Fig. 1 Normalized dc electrical resistivities versus temperature interval 90–115 K for pure and Ni surface-layered Bi-2223 superconducting ceramics prepared at different diffusion annealing temperature between 650 and 850 °C. Inset: Original experimental dc resistivities as a function of temperature for the polycrystalline ceramic materials

of materials. According to the inset of Fig. 1, it is clear that the change in the annealing temperature affects remarkably the resistivity curves of materials studied in this work except for the truly-metallic behavior. This is attributed to the logarithmic divergence of the densities of active and dynamic electronic states (related to the electron–phonon interactions in the Cu–O₂ consecutively stacked layers) at the vicinity of Fermi energy level [31–33]. In other words, the bulk superconducting materials each exhibit positively linear temperature dependence of electrical resistivity ($dp/dt > 0$) in the normal state as a result of the intrinsic truly-metallic feature (correlated with Matthiessen’s rule, $\rho_T = \rho_{res} + \rho_{i_T}$) during the electrical transition from normal state into the superconducting state [34]. In relation of Matthiessen’s rule, the total resistivity (abbreviated as ρ_T) consists of two main parts: (I) the temperature-dependent resistivity (ρ_{i_T}) is directly related to the environmental temperature and changes at any temperature values; (II) the residual resistivity (ρ_{res}) received to be opposite of conductivity nature is not the first order temperature-dependent term and can be changed by the presence of omnipresent flaws and structural defects (point, line, planar or bulk) throughout the Cu–O₂ consecutively stacked sheets in the crystal structure [35]. In the present work, the intercept of extrapolation of electrical resistivity values to zero on the temperature axis enables us to determine the ρ_{res} parameters for every material. In this respect, the Ni-700 sample with the smallest residual resistivity (0.05 mΩ cm) obtains the minimum defects whereas the Ni-850 sample with the highest residual resistivity value of 2.06 mΩ cm presents the worst material quality due to the increased permanent defects, omnipresent flaws (stress raisers and crack initiation sites), distortions, disorders in the orientation of adjacent layers and the connectivity coupling problems between the grains in the crystal structure [36, 37]. To sum up, the major result with the truly-metallic scenario obtained from Fig. 1 is the fact that the metallic behavior systematically develops with increasing the diffusion annealing temperature until such a certain value of 700 °C above which the truly-metallic character falls into the decrement trend. When the diffusion annealing temperature is in the maximum (excess) point of 850 °C, the metallic character is damaged significantly because of the enhanced structural problems, the densities of active and dynamic electronic states, σ gap anisotropy and electron–phonon interactions as they do.

As for the second noteworthy characteristic parameter: normal state resistivity values at 300 K, the diffusion annealing temperature up to the critical value of 700 °C affects positively the metallic connections between the superconducting grains along with the consecutively stacked layers in the Bi-2223 crystal system due to the formation of more homogeneous regions (the considerable decrement of coupling boundary problems) and stabilization and (degradation

of structural problems in the crystal matrix). In this respect, the optimum annealing temperature results in more formation of effective electron–phonon coupling probabilities (percentage of clusters in the superconducting path) and the mobile hole carrier concentration gets more and more optimized [38]. Conversely, the excess annealing temperature value (introduction of excess Ni foreign impurities to the crystal structure [26, 27]) augments the interaction coupling problems between the isolated grains (meaning the break of both homogeneous regions and stabilization). Shortly, the metallic characteristics of polycrystalline ceramics studied are demolished considerably. Numerically, the normal state resistivity of pure material at the room temperature is observed to be about 7.25 mΩ cm (Table 1). The increment in the metallic connectivity with the annealing temperature up to the value of 700 °C truncates the ρ_{300K} value towards to the value of 5.56 mΩ cm as given in Table 1. This is in association with the fact that the optimum diffusion annealing temperature (leading to penetration of the optimum Ni impurities into the crystal texturing) improves significantly the coupling probability between isolated superconducting grains. However, the resistivity value increases again to 11.24 mΩ cm, which is the global maximum point for the normal state resistivity value at the room temperature. The long and short of it is that highly conductive (1.4×10^7 S/m) Ni host-impurities embedded in the crystal lattice favor the electrical properties of the Bi-2223 system on the condition of optimum annealing temperature (700 °C for the Ni surface-layered bulk Bi-2223 superconducting system).

The parameters of RRR , ρ_{norm} , ρ_{115K} and $\Delta\rho$ are another results deduced from the dc electrical resistivity measurements. In advance, the RRR parameter is in accordance with the material quality (deformation and bond strength in the crystal lattice) and described to be the ratio of ρ_{300K}/ρ_{115K} [39]. According to the experimental evidences, the RRR parameters tend to increase from 3.42 until 7.32 with ascending the diffusion annealing temperature up to the critical temperature value of 700 °C beyond which the RRR constant begins to decrease monotonously and in fact locating in the global minimum value of 2.23 for the

Ni-850 compound (Table 1). This is in association with the fact that the optimum diffusion annealing temperature of 700 °C augments the sample quality and bond strength in the crystal matrix. From the critical annealing temperature value of 700 °C onwards, the coupling boundary problems, omnipresent flaws and especially structural problems are observed to harm the electrical properties of Ni surface-layered Bi-2223 superconducting materials.

Further, the parameter of ρ_{115K} ascribes to the existence of crack-producing flaws, impurity scattering and lattice strains through the crystal structure. As for the experimental values ranging from 0.71 to 5.02 mΩ cm (Table 1), the former (minimum) parameter of 0.71 mΩ cm is attributed to the Ni-700 superconducting ceramic whereas the Ni-850 material exhibits the latter (maximum) value of 5.02 mΩ cm. Besides, the ρ_{115K} parameter is found to be about 2.07 mΩ cm for the pristine sample. This is in correspondence to the fact that the omnipresent flaws (known as the stress raisers and crack initiation sites), impurity scattering and lattice strains considerably diminish with the increment of the diffusion annealing temperature up to 700 °C after which the structural problems begin to increase suddenly again and reach to the maximum points.

Additionally, we are interested in the other crucial parameters of $\Delta\rho = \rho_{300K} - \rho_{115K}$ and $\rho_{norm} = \rho_{115K}/\Delta\rho$ that are related to the metallic characteristic and crystal quality. In the current work, the Ni-700 superconducting sample exhibits the minimum $\Delta\rho$ of 4.80 mΩ cm and ρ_{norm} of 0.16 whereas the maximum values of 6.20 mΩ cm and 0.59 are attributed to the Ni-850 inorganic compound. Thus, it is just this last descriptor that is a clue for the degradation of metallic characteristic and crystal quality in case of the excess diffusion annealing temperature.

Moreover, one can encounter the effect of diffusion annealing temperature ($650 \leq T \leq 850$ °C) on the critical transition temperatures (onset, T_c^{onset} and offset, T_c^{offset}) of the pure and Ni diffusion-doped Bi-2223 superconducting materials with the aid of experimental dc resistivity curves as displayed in Fig. 1. In case of the former (T_c^{onset}) temperature, the isolated superconducting grains transit

Table 1 Detailed electrical resistivity results (onset and offset critical transition temperatures, room temperature resistivities, residual resistivities, residual resistivity ratios, ΔT_c , ρ_{115K} , ρ_{norm} and $\Delta\rho$ parameters) belonging to the bulk superconductors

Samples	ρ_{300K} (mΩ cm)	ρ_{115K} (mΩ cm)	RRR (ρ_{300K}/ρ_{115K})	$\Delta\rho$ ($\rho_{300K} - \rho_{115K}$) (mΩ cm)	ρ_{norm} ($\rho_{115K}/\Delta\rho$)	ρ_{res} (mΩ cm)	T_c^{onset} (K)	T_c^{offset} (K)	ΔT_c (K)
Virgin	7.25	2.09	3.47	5.16	0.41	0.72	110.34	108.23	2.11
Ni-650	6.32	1.35	4.68	4.97	0.27	0.32	110.74	109.55	1.19
Ni-700	5.56	0.76	7.32	4.80	0.16	0.05	112.18	111.35	0.83
Ni-750	8.74	2.72	3.21	6.02	0.45	1.02	109.55	105.47	4.08
Ni-800	9.76	3.60	2.71	6.16	0.59	1.42	108.59	101.23	7.36
Ni-850	11.24	5.04	2.23	6.20	0.81	2.06	107.53	97.46	10.07

into the superconducting state and hence the formation of electron–phonon coupling drives the superconductivity. On the other hand, the latter critical temperature being the responsible for the features of inter-granular component is related to the different volume phase fractions appeared in the crystal system [40]. After the T_c^{offset} value, the material exhibits totally superconducting behavior. Besides, the T_c^{onset} value is always higher than the T_c^{offset} value. In the current work, the diffusion annealing temperature affects sensitively both the temperature values (especially T_c^{offset}). According to the experimental findings, it suffices to confirm that the annealing temperature more affects the features of inter-granular component in comparison with the formation of electron–phonon coupling or cooper-pairs. Similarly, it is believed that the optimum annealing ambient leads to harshly improve the homogeneities in the oxidation states, mobile hole concentration, σ gap anisotropy, orientations of adjacent layers, connectivity coupling problems, electron–phonon interactions, densities of electronic states and structural problems [41, 42]. The value of 700 °C is, in this respect, observed to be the optimum diffusion annealing temperature for the Ni surface-layered Bi-2223 superconducting crystal structure.

The orientations of Cu–O₂ consecutively stacked layers with higher mobile hole concentration and homogeneities in the oxidation states develop with enhancement in the diffusion annealing temperature up to 700 °C above which not only do the layers get more and more misorientated, but the mobile hole concentration level and oxidation state homogeneities deviate from the optimum values, as well. In more sophisticatedly, in case of the optimum temperature of 700 °C (resulting in the optimum Ni impurity penetration into the Bi-2223 crystal matrix), intrinsically over-doped nature of Bi-based superconducting system transits into optimally doped state (optimum level of electron–phonon coupling) [43]. However, the excess annealing temperature (after the critical temperature value of 700 °C) makes the optimum doping state reside in the underdoped state position for the Ni diffusion-doped (hole-induced) Bi-2223 compound. The main reason of deviation in the optimization stems from the localization (metastability) of density of active and dynamic electronic states at the Fermi energy level [44, 45]. In other words, the hole trap energy levels within the small energy intervals of mobile holes (being association with the order parameter of super-electrons) degrade significantly [46]. Moreover, it is necessary to underline that the excess introduction of Ni foreign impurities into the crystal lattice damages both the overlapping in the wave functions (hybridization mechanism) of Cu 3d-O 2p orbitals [43] and the amplitude of pair wave function ($\Psi = \Psi_0 e^{-i\varphi}$, here Ψ_0 parameter ascribes to number of super-electrons) [46].

As for the phenomenological interpretation of differentiation in the T_c^{onset} and T_c^{offset} parameters for the Bi-2223 ceramics, the optimum incorporation of Ni impurities into the crystal structure hardens suddenly the O(2)SrA1g phonon; conversely, the O(1)CuA1g and B1g phonons soften extensively due to the regression of both the internal pressure and oxygen level (valency) in the Bi–O double layers [47]. Similarly, the optimum diffusion annealing temperature enhances the vibrational mode intensities of the atoms in adjacent layers as a consequence of the reduced metallic screening in the hole-induced Bi-2223 inorganic compounds. In conclusion, all the mechanisms given above are able to explain that why the diffusion annealing temperature changes the critical transition temperatures. In our research for this paper, the T_c^{onset} values are found to change from about 107.53 K (for the worst sample of Ni-850) to 112.18 K (for the best sample of Ni-700) whereas the maximum (minimum) T_c^{offset} value is observed to be about 111.35 K (97.46 K) for the Ni-700 (Ni-850) material. The pure sample presents the T_c^{onset} and T_c^{offset} values of 110.34 and 108.23 K, respectively. Additionally, the changes between T_c^{onset} and T_c^{offset} values (known as broadening degree, $\Delta T_c = T_c^{onset} - T_c^{offset}$) allow us to determine the practicability of Ni inclusions for the industrial, engineering and large scale applications of Bi-2223 inorganic ceramic materials. In this respect, the smallest ΔT_c value of nearly 0.83 K is noted for the Ni-700 material when the Ni-850 ceramic obtains the largest ΔT_c value of nearly 10.07 K. Hence, the change of ΔT_c verifies the fact that the annealing temperature of 700 °C is the alluring value for the applications of Ni surface-layered bulk Bi-2223 superconductors. This is another probable result obtained from the degree of broadening that the optimum penetration of Ni individuals into the Bi-2223 crystal matrix promotes seriously the purity of Bi-2223 phase.

3.2 Calculation of diffusion coefficient and required activation energy of Ni impurities for Bi-2223 superconducting system

In this part of paper, we examine the temperature-dependent diffusivity and required activation energy of heavy metal ions of nickel to penetrate into the Bi-2223 crystal matrix for the first time. For this purpose, firstly we determine the diffusivity of Ni foreign impurities along the Bi-2223 crystal structure for all the samples via the changes of electrical resistivity curves versus thickness values after the thin-layer removal from the material surface (showing the similar features with the concentration distribution of the diffused impurity). Then, the appropriate error function enables us to find the temperature-dependent diffusion coefficient of Ni impurities in the Bi-2223 lattice system so that we understand the relationship between the Ni diffusivity and annealing temperature. Finally, the required minimum activation

energy value for the penetration of the heavy metal ions of nickel impurities into the polycrystallized Bi-2223 superconducting crystal lattice by using the Arrhenius relation for the first time. According to the equations provided in the part of experimental measurement details and computational approaches, the differentiation of dc electrical resistivity

parameters $\Delta\rho/\rho_0$ (ρ_0 presents the electrical resistivity of pure region) with regard to the thin-layer removal thickness from the sample surface for all the materials prepared are displayed in Fig. 2 in detail. In the graphics given, the solid curve is attributed the concentration profile of Ni impurities diffused into the Bi-2223 superconducting crystal system.

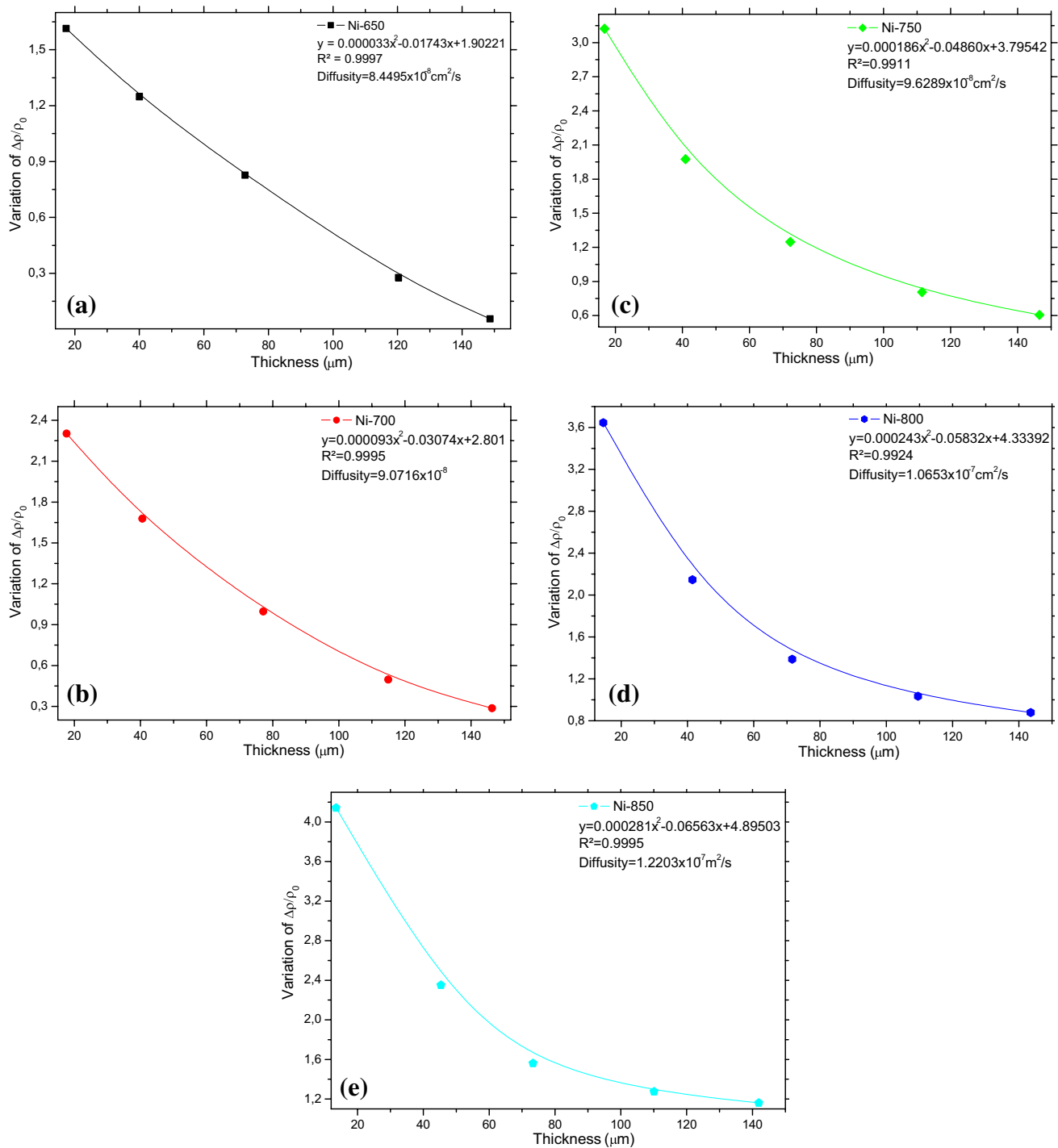


Fig. 2 Variation of dc electrical resistivity parameters $\Delta\rho/\rho_0$ against thin-layer removal thickness from the sample surface for **a** Ni-650, **b** Ni-700, **c** Ni-750, **d** Ni-800 and **e** Ni-850 ceramic compound

Table 2 Ni diffusion fast-rates and fitting parameters of diffusion coefficients with regard to annealing temperature for every solid Bi-2223 ceramic

Diffusion-annealing temperature (°C)	Diffusion coefficient ($\text{cm}^2 \text{s}^{-1}$)	Diffusivity based on diffusion annealing temperature
650	8.4495×10^{-8}	3.28×10^{-5}
700	9.0716×10^{-8}	9.31×10^{-5}
750	9.6289×10^{-7}	1.86×10^{-4}
800	1.0653×10^{-7}	2.43×10^{-4}
850	1.2203×10^{-7}	2.81×10^{-4}

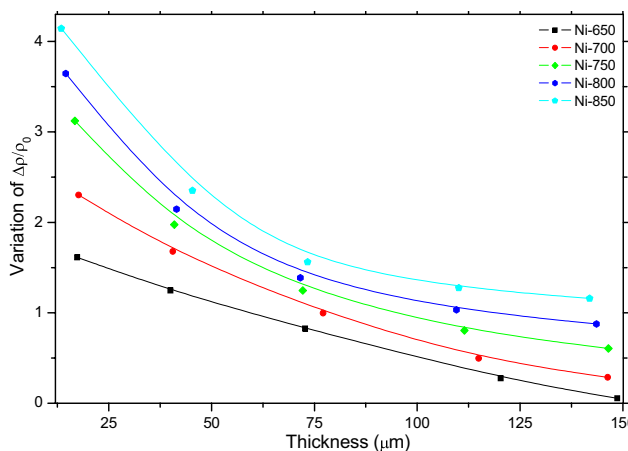


Fig. 3 Dc electrical resistivity variation curves for every ceramic sample

On the condition that the experimental results observed fit very well with the theoretical curves drawn, the diffusion fast-rate belonging to the Ni impurity is perfectly satisfied by Eqs. 1 and 2. Thus, in the diffusion annealing temperature range from 650 to 850 °C the diffusion coefficients for the Ni foreign impurity through the consecutively stacked layers in the Bi-2223 crystal system are calculated to be about 8.4495×10^{-8} , 9.0716×10^{-8} , 9.6289×10^{-7} , 1.0653×10^{-7} and $1.2203 \times 10^{-7} \text{ cm}^2 \text{ s}^{-1}$. The values are arranged according to the increment trend of annealing temperature (Table 2). In this respect, it is fair to conclude that the diffusion coefficient enhances systematically with increasing the diffusion annealing temperature, and hence, the excess annealing temperature makes the Ni impurities more and more penetrate into the isolated superconducting grains. We also gather the resistivity variation curves for every sample in Fig. 3 to achieve more detailed knowledges about the temperature effect on the diffusivity. It is clear that for all the superconducting samples produced in this work the dc electrical resistivity initially alters (decreases) rapidly with the thin-layer removal thickness from the specimen surface. The decrement trend lowers constantly with the increment in the layer thickness, and in fact reaches to the

global minimum value in case of the deepest points in the materials (especially Ni-850 sample). This is attributed to fact that the diffusion of nickel impurities into the Bi-2223 crystal structures is perfectly performed in the current study. It is another probable result deduced from this work that we examine the curves (related to the change of dc electrical resistivity values as a function of the thin-layer removal thickness from the sample surface) in Fig. 3 with the aid of the fitting equations deduced from the quadratic formulas. The fitting parameters determined are tabulated in Table 2. According to the table, the diffusivity based on the diffusion annealing temperature (variation of x^2) is found to increase systematically from 3.28×10^{-5} to 2.81×10^{-4} with ascending the annealing temperature from 650 to 850 °C. One might logically confirm from the table that after the critical diffusion annealing temperature such a value of 700 °C the nickel nanoparticles begin to incorporate into both into the superconducting grains and over the grain boundaries along with the Bi-2223 crystal lattice. In case of the maximum diffusion annealing temperature, the nickel impurities predominantly accumulate over the grain boundaries [48, 49]. This fact can also be deduced from the tail part (as the removal thickness of $\sim 150 \mu\text{m}$) of $\Delta\rho/\rho_0$ curve presenting the both the most parabolic and highest values. In other words, the excess annealing temperature demonstrates still the presence of Ni impurities in the Ni-850 sample with the highest differentiation in the dc electrical resistivity. This gives a pictorial representation of experimental dc electrical resistivity measurement results part in the paper. All in all, the diffusion fast-rate is found to be strongly dependent upon the diffusion annealing temperature. In fact, it is reasonable to conclude that the diffusion coefficients evaluated begin much more significant at higher diffusion annealing temperatures in comparison with those at lower ones.

Based on both parts (experimental dc electrical resistivity measurement results and calculation of diffusion fast-rate and required activation energy of Ni impurities for Bi-2223 superconducting system) in the paper, it is pertinent to mention here that the Ni concentration primarily improves exhaustively the structural problems, omnipresent flaws, coupling boundary problems, adjacent layer orientations, mobile hole concentration, electron–phonon interactions, homogeneities in the oxidation states and densities of active and dynamic electronic states in the bulk Bi-2223 polycrystalline compounds until the critical diffusion annealing temperature value of 700 °C, beyond which the excess annealing temperature leads to the nickel impurities accumulate predominantly over the grain boundaries. Thus, the refinement mechanism becomes reversed as a consequence of excess Ni penetration into the Bi-2223 crystal system.

At the same time, we survey sensitively the temperature-dependent diffusion coefficient parameter of Ni impurity for the Bi-2223 superconducting crystal system

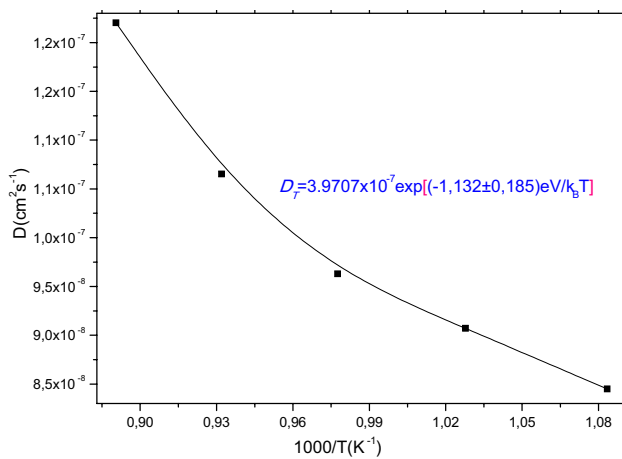


Fig. 4 Temperature-dependent Ni diffusion fast-rate in the vicinity of specimen surface at the temperatures between 650 and 850 °C for the bulk Bi-2223 ceramic materials

via the mean diffusion fast-rates by using the Arrhenius relation to define the relationship between the Ni diffusivity and diffusion annealing temperature (Fig. 4). One can observe the temperature-dependent Ni diffusion rate-fast of $3.9707 \times 10^{-7} \text{ cm}^2 \text{ s}^{-1}$ in the vicinity of specimen surface at the temperatures between 650 and 850 °C for the bulk Bi-2223 ceramic materials. Besides, Fig. 4 shows the activation energy value of 1.132 eV that is required minimum energy parameter for the penetration of nickel impurities into the bulk Bi-2223 crystal lattice. According to the combination of relatively low temperature-dependent diffusion coefficient and high activation energy parameters inferred from the Arrhenius equation, the required minimum activation energy for the introduction of heavy metal Ni ions to the Bi-2223 crystal structure is 1.132 eV.

4 Conclusion

The present work is aim both to define two fundamental physical quantities (temperature-dependent diffusion coefficient and required activation energy) for the incorporation of Ni foreign impurities into the Bi-2223 superconducting crystal system, and to shed some lights on the variation of electrical and superconducting properties of Ni surface-layered Bi-2223 superconducting ceramics prepared by the solid-state reaction method. For the calculation of the temperature-dependent diffusion coefficients [$D = D_0 \exp(E/k_B T)$] for the nickel particles, the diffusion fast-rates belonging to every material produced at the different annealing temperature range of 650–850 °C are obtained by the changes of dc electrical resistivity parameters $\Delta\rho/\rho_0$ with regard to the thin-layer removal thickness by means of error function. Similarly, the required minimum activation energy for

the incorporation of Ni particles into the polycrystallized Bi-2223 crystal system is determined by the Arrhenius equation. Moreover, we survey the role of diffusion annealing temperature on the electrical and superconducting characteristic properties regarding the room temperature resistivities, residual resistivities, residual resistivity ratios, onset and offset critical transition temperatures, $\rho_{115\text{K}}$, ρ_{norm} , and $\Delta\rho$ quantities of Ni surface-layered bulk Bi-2223 superconducting materials. Taking into account all the experimental results provided above, the variations in the fundamental physical quantities inferred from this study are as follows:

- All the results discussed in the present work display that the optimum annealing temperature (leading to the incorporation of optimum Ni concentration level into the crystal lattice) of 700 °C improves thoroughly the formation of effective electron–phonon coupling or cooper-pair probabilities (percentage of clusters in the superconducting path), homogeneities in the oxidation states, mobile hole concentration, σ gap anisotropy, densities of active and dynamic electronic states, orientations of adjacent layers, interaction coupling boundary problems, omnipresent flaws and structural problems in the bulk Bi-2223 superconducting material. In this respect, the optimum diffusion annealing temperature is observed to be 700 °C for the electrical and superconducting characteristics.
- Moreover, the dc electrical resistivity measurements demonstrate that the bulk ceramic material exposed to 700 °C annealing temperature shows not only the smallest $\rho_{300\text{K}}$, ρ_{res} , $\rho_{115\text{K}}$, ρ_{norm} , $\Delta\rho$ and ΔT_c quantities, but also the highest truly-metallic behavior, conductivity, stabilization of superconductivity in the more homogeneous regions, overlapping of Cu-3d and O-2p wave functions (hybridization mechanism), amplitude of pair wave function, formation of cooper-pairs, RRR (sample quality and bond strength in the crystal matrix), T_c^{onset} and T_c^{offset} parameters.
- For every material the variation $\Delta\rho/\rho_0$ trend decreases considerably in with the increment of the thin-layer removal thickness from the surface, and in fact dwells in the global minimum differentiation in case of the deepest points in the material. What stands out clearly here is that the diffusion of Ni impurities into the bulk Bi-2223 crystal system is perfectly exerted in the present study.
- Based on the error function computations, the diffusion coefficient parameter of Ni foreign impurities is found to increase monotonously from 8.4495×10^{-8} to $1.2203 \times 10^{-7} \text{ cm}^2 \text{ s}^{-1}$ with the enhancement of diffusion annealing temperature. This is in attribution to the fact that the annealing temperature causes to penetrate more and more Ni impurities into the isolated superconducting grains. In other words, the diffusion coefficients seem

to be much more significant at rather higher annealing temperatures as compared to lower temperatures.

- Furthermore, the fitting equations (in the quadratic forms) deduced from the variation $\Delta\rho/\rho_0$ curves confirm that from higher annealing temperature such a value of 700 °C onwards, the nickel impurities begin to enter both into the isolated superconducting grains and predominantly over the grain boundaries throughout the Bi-2223 crystal structure. In fact, the nickel impurities begin to accumulate predominantly over the grain boundaries. Thus, the excess annealing temperatures damage significantly the electrical and superconducting properties.
- At the same time, the temperature-dependent Ni diffusivity is found to be $D = 3.9707 \times 10^{-7} \exp[(-1.132 \text{ eV}/k_B T)]$ of nickel particles at the specimen surface of the bulk Bi-2223 ceramic compound. In this respect, the diffusivity is noted to be about $3.9707 \times 10^{-7} \text{ cm}^2 \text{ s}^{-1}$ when the corresponding minimum activation energy for the penetration of heavy metal Ni ions into the bulk Bi-2223 crystal structure is calculated to be about 1.132 eV. The major reason related with the combination of relatively low temperature-dependent diffusion coefficient and high activation energy value presents that the heavy metal Ni ions are hard put to penetrate into the Bi-2223 crystal structure.
- As for the excess diffusion annealing temperature, the Bi-2223 crystal system diverges from the optimally doped state (optimum level of electron–phonon coupling) towards to the underdoped state position. Thus, the density of active and dynamic electronic states at the Fermi energy level localize (metastability) suddenly, accordingly the electrical and superconducting properties damage seriously. This is at least equally important of the increased interaction coupling boundary problems, omnipresent flaws and structural problems with the excess annealing temperature.

Acknowledgements This study is totally supported by Abant Izzet Baysal University Scientific Research Project Coordination Unit (Project No: 2014.09.05.685).

References

1. S.Y. Oh, H.R. Kim, Y.H. Jeong, O.B. Hyun, C.J. Kim, Joining of Bi-2212 high-T_c superconductors and metals using indium solders. *Physica C* **463**, 464–467 (2007)
2. M. Chen, W. Paul, M. Lakner, L. Donzel, M. Hoidis, P. Untermaier, R. Weder, M. Mendik, 6.4 MVA resistive fault current limiter based on Bi-2212 superconductor. *Physica C* **372**, 1657–1663 (2002)
3. J.D. Hodge, H. Muller, D.S. Applegate, Q. Huang, A resistive fault current limiter based on high temperature superconductors. *Appl. Supercond.* **3**, 469–482 (1995)
4. V.L. Ginzburg, E.A. Andryushin, *Superconductivity*, Revised edn. World Scientific Pub. Co. Inc. (2004)
5. G. Yildirim, Determination of optimum diffusion annealing temperature for Au surface-layered Bi-2212 ceramics and dependence of transition temperatures on disorders. *J. Alloy. Compd.* **699**, 247–255 (2017)
6. A.M. Hermann, J.V. Yakhmi eds., *Thallium-Based High-Temperature Superconductors*. (Marcel Dekker, New York, 1994)
7. N.K. Saritekin, M. Dogruer, Y. Zalaoglu, G. Yildirim, C. Terzioğlu, O. Gorur, Filling of electronic density of states in Y-123 superconducting ceramics by nano Nd substitution on Ba site in crystal structure. *J. Alloy. Compd.* **659**, 31–37 (2016)
8. B. Batlogg, Cuprate superconductors: science beyond high T_c. *Solid State Commun.* **107**, 639–647 (1998)
9. O. Gorur, Y. Ozturk, G. Yildirim, M. Dogruer, C. Terzioğlu, Sn diffusion coefficient and activation energy determined by way of XRD measurement and evaluation of micromechanical properties of Sn diffused YBa₂Cu₃O_{7-x} superconducting ceramics. *J. Mater. Sci.: Mater. El* **24**, 3063–3072 (2013)
10. N.K. Saritekin, M. Pakdil, E. Bekiroğlu, G. Yildirim, Examination of effective nucleation centers for flux pinning of vortices and optimum diffusion annealing temperature for Au-diffusion-doped Bi-2212 polycrystalline compound. *J. Alloy. Compd.* **688**, 637–646 (2016)
11. S. Nagaya, N. Hirano, M. Naruse, T. Watanabe, T. Tamada, Development of a high-efficiency conduction cooling technology for SMES coils. *IEEE T. Appl. Supercond.* **23**, 5602804–5602807 (2013)
12. M. Runde, Application of high-T_c superconductors in aluminum electrolysis plants. *IEEE T. Appl. Supercond.* **5**, 813–816 (1995)
13. T.A. Coombs, A finite element model of magnetization of superconducting bulks using a solid-state flux pump. *IEEE T. Appl. Supercond.* **21**, 3581–3586 (2011)
14. F.N. Werfel, U. Floegel-Delor, R. Rothfeld, T. Riedel, B. Goebel, D. Wippich, P. Schirrmeister, Superconductor bearings, flywheels and transportation. *Supercond. Sci. Technol.* **25**, 014007 (2012)
15. H.H. Xu, L. Cheng, S.B. Yan, D.J. Yu, L.S. Guo, X. Yao, Recycling failed bulk YBCO superconductors using the NdBCO/YBCO/MgO film-seeded top-seeded melt growth method. *J. Appl. Phys.* **111**, 103910 (2012)
16. K.Y. Choi, I.S. Jo, S.C. Han, Y.H. Han, T.H. Sung, M.H. Jung, G.S. Park, S.I. Lee, High and uniform critical current density for large-size YBa₂Cu₃O_{7-δ} single crystals. *Curr. Appl. Phys.* **11**, 1020–1023 (2011)
17. W. Buckel, R. Kleiner, *Superconductivity: Fundamentals and Applications*, 2nd edn. (Wiley-VCH Verlag, Weinheim, 2004)
18. H. Miao, M. Meinesz, B. Czabai, J. Parrell, S. Hong, Microstructure and J_c improvements in multifilamentary Bi-2212/Ag wires for high field magnet applications. *AIP Conf. Proc.* **986**, 423–430 (2008)
19. K. Koyama, S. Kanno, S. Noguchi, Electrical, Magnetic and superconducting properties of the quenched Bi₂Sr₂Ca_{1-x}Nd_xCu₂O_{8+y} system. *Jpn. J. Appl. Phys.* **29**, L53–L56 (1990)
20. L. Zhou, P. Zhang, P. Ji, K. Wang, X. Wu, The properties of YBCO superconductors prepared by a new approach—the powder melting process. *Supercond. Sci. Technol.* **3**, 490–492 (1990)
21. K. Salama, V. Selymanickam, L. Gao, K. Sun, High-current density in bulk YBa₂Cu₃O_x superconductor. *Appl. Phys. Lett.* **54**, 2352–2354 (1989)
22. T. Egi, J.G. Wen, K. Kuroda, H. Unoki, N. Koshizuka, High-current density of Nd(Ba,Nd)₂Cu₃O_{7-x} single-crystal. *Appl. Phys. Lett.* **67**, 2406–2408 (1995)
23. S. Jin, T.H. Tiefel, R.C. Sherwood, M.E. Davis, R.B. Van Dover, G.W. Kammlott, R.A. Fasnacht, H.D. Keith, High critical currents in Y-Ba-Cu-O superconductors. *Appl. Phys. Lett.* **52**, 2074–2076 (1988)

24. J.M. Hur, K. Togano, A. Matsumoto, H. Kumakura, H. Wada, K. Kimura, Fabrication of high-performance MgB_2 wires by an internal Mg diffusion process. *Supercond. Sci. Technol.* **21**, 032001 (2008)
25. P. Grathwohl, *Diffusion in Natural Porous Media: Contaminant Transport, Sorption/desorption and Dissolution Kinetics*. (Kluwer Academic, Boston, 1998)
26. N.K. Saritekin, H. Bilge, M.F. Kahraman, Y. Zalaoglu, M. Pakdil, M. Dogruer, G. Yildirim, M. Oz, Improvement of mechanical characteristics and performances with Ni diffusion mechanism throughout Bi-2223 superconducting matrix. *AIP Conf. Proc.* **1722**, 140002 (2016)
27. N.K. Saritekin, M.F. Kahraman, H. Bilge, Y. Zalaoglu, M. Pakdil, M. Dogruer, G. Yildirim, M. Oz, Effect of Ni diffusion annealing temperature on crucial characterization of Bi-2223 superconducting system. *AIP Conf. Proc.* **1722**, 140007 (2016)
28. A. Fick, Ueber diffusion. *Ann. der Physik* **94**, 59–86 (1855)
29. G.B. Abdullaev, T.D. Dzhaferov, *Atomic Diffusion in Semiconductor Structures*, 2nd edn. (Harwood, Chur, 1987)
30. R.B. Bird, W.E. Stewart, E.N. Lightfoot, *Transport Phenomena*. (Wiley-Blackwell, New York, 1976)
31. P.B. Allen, W.E. Pickett, H. Krakauer, Anisotropic normal-state transport-properties predicted and analyzed for high- T_c oxide superconductors. *Phys. Rev. B* **37**, 7482–7490 (1988)
32. D.M. Newns, P.C. Pattnaik, C.C. Tsuei, Role of vanhove singularity in high-temperature superconductors-Mean field. *Phys. Rev. B* **43**, 3075–3084 (1991)
33. S. Martin, M. Gurvitch, C.E. Rice, A.F. Hebard, P.L. Gammel, R.M. Fleming, A.T. Fiory, Nonlinear temperature-dependence of the normal-state resistivity in $\text{YBa}_2\text{Cu}_4\text{O}_{8+\delta-\gamma}$ films. *Phys. Rev. B* **39**, 9611–9613 (1989)
34. J. Ekin, *Experimental Techniques for Low-Temperature Measurements: Cryostat Design, Material Properties and Superconductor Critical-Current Testing*. (Oxford University Press, New York, 2006)
35. M. Li, Y. Zhang, Y. Li, Y. Qi, Granular superconductivity in polycrystalline $\text{Bi}_2\text{Sr}_2\text{CaCu}_2\text{O}_{8+\gamma}$ by homovalent La substitution on Bi sites. *J. Non-Cryst. Solids* **356**, 2831–2835 (2010)
36. N.Y. Chen, R. Jonker, V.C. Matijasevic, H.M. Jaeger, J.E. Mooij, Low 1/f normal-state resistance noise in high-resistivity $\text{YBa}_2\text{Cu}_3\text{O}_y$ films. *Appl. Phys. Lett.* **67**, 133–135 (1995)
37. F. Rullier-Albenque, P.A. Vieillefond, H. Alloul, A.W. Tyler, P. Lejay, J.F. Marucco, Universal T_c depression by irradiation defects in underdoped and overdoped cuprates. *Europhys. Lett.* **50**, 81–87 (2000)
38. M.B. Turkoz, S. Nezir, C. Terzioglu, A. Varilci, G. Yildirim, Investigation of Lu effect on $\text{YBa}_2\text{Cu}_3\text{O}_{7-\gamma}$ superconducting compounds. *J. Mater. Sci: Mater. El* **24**, 896–905 (2013)
39. X. Xu, J.H. Kim, S.X. Dou, S. Choi, J.H. Lee, H.W. Park, M. Rindfleish, M. Tomsic, A correlation between transport current density and grain connectivity in MgB_2/Fe wire made from ball-milled boron. *J. Appl. Phys.* **105**, 103913 (2009)
40. R. Awad, A.I. Abou-Aly, M.M.H. Abdel Gawad, I. G-Eldeen, The influence of SnO_2 nano-particles addition on the vickers micro-hardness of (Bi, Pb)-2223 superconducting phase. *J. Supercond. Nov. Magn.* **25**, 739–745 (2012)
41. D.M. Rao, T. Somaiah, V. Haribabu, Y.C. Venudhar, Growth-kinetics of high- T_c and low- T_c phases in $\text{Bi}_{2-x}\text{Pb}_x\text{Ca}_2\text{Sr}_2\text{Cu}_3\text{O}_y$ superconducting compounds. *Cryst. Res. Technol.* **28**, 285–298 (1993)
42. A. Ianculescu, M. Gartner, B. Despax, V. Bley, Th Lebey, R. Gavrila, M. Modreanu, Optical characterization and microstructure of BaTiO_3 thin films obtained by RF-magnetron sputtering. *Appl. Surf. Sci.* **253**, 344–348 (2006)
43. X.L. Lin, S.S. Ma, H.Y. Wang, H. Xu, Characteristics of hopping conductivity in one-dimensional binary disordered system with off-diagonal correlations. *Acta Phys. Sin* **56**, 2852–2857 (2007)
44. G. Yildirim, Beginning point of metal to insulator transition for Bi-2223 superconducting matrix doped with Eu nanoparticles. *J. Alloy. Compd.* **578**, 526–535 (2017)
45. H. Eskes, G.A. Sawatzky, Tendency towards local spin compensation of holes in the high- T_c copper-compounds. *Phys. Rev. Lett.* **61**, 1415–1418 (1988)
46. M. Pakdil, E. Bekiroglu, M. Oz, N.K. Saritekin, G. Yildirim, Role of preparation conditions of Bi-2223 ceramic materials and optimization of Bi-2223 phase in bulk materials with experimental and statistical approaches. *J. Alloy. Compd.* **673**, 205–214 (2016)
47. M. Kakihana, M. Osada, M. Kall, L. Borjesson, H. Mazaki, H. Yasuoka, M. Yashima, M. Yoshimura, Raman-active phonons in $\text{Bi}_2\text{Sr}_2\text{Ca}_{1-x}\text{Y}_x\text{Cu}_2\text{O}_{8+\delta}$ ($x = 0-1$): Effects of hole filling and internal pressure induced by Y doping for Ca, and implications for phonon assignments. *Phys. Rev. B* **53**, 11796–11806 (1996)
48. M. Dogruer, O. Gorur, F. Karaboga, G. Yildirim, C. Terzioglu, Zr diffusion coefficient and activation energy calculations based on EDXRF measurement and evaluation of mechanical characteristics of $\text{YBa}_2\text{Cu}_3\text{O}_{7-x}$ bulk superconducting ceramics diffused with Zr nanoparticles. *Powder Technol.* **246**, 553–560 (2013)
49. M. Dogruer, G. Yildirim, E. Yucel, C. Terzioglu, Role of diffusion-annealing temperature on the microstructural and superconducting properties of Cu-doped MgB_2 superconductors. *J. Supercond. Nov. Magn.* **23**, 1965–1970 (2012)